CHEMISTRY
A EUROPEAN JOURNAL

DOI: 10.1002/chem.200500280

Preparation, Structure, and Ethylene Polymerization Behavior of Half-Sandwich Picolyl-Functionalized Carborane Iridium, Ruthenium, and Rhodium Complexes

Xin Wang and Guo-Xin Jin*[a]

Dedicated to Professor Dr. Herbert Schumann on the occasion of his 70th birthday

Abstract: The synthesis of half-sandwich transition-metal complexes containing the $\mathrm{Cab^N}$ and $\mathrm{Cab^{N,S}}$ chelate ligands ($\mathrm{HCab^N = HC_2B_{10}H_{10}CH_2C_5H_4N}$ (**1**), $\mathrm{LiCab^{N,S} = LiSC_2B_{10}H_{10}CH_2C_5H_4N}$ (**4**)) is described. Compounds **1** and **4** were treated with chloride-bridged dimers $[\{\mathrm{Ir(Cp^*)Cl_2}\}_2]$ ($\mathrm{Cp^* = \eta^5\text{-}C_5Me_5}$), $[\{\mathrm{Ru}(p\text{-cymene})\mathrm{Cl_2}\}_2]$ and $[\{\mathrm{Rh(Cp^*)Cl_2}\}_2]$ to give half-sandwich complexes $[\mathrm{Ir(Cp^*)Cl(Cab^N)}]$ (**2**), $[\mathrm{Ru}(p\text{-cymene})\mathrm{Cl(Cab^N)}]$ (**3**), and $[\mathrm{Rh(Cp^*)Cl(Cab^{N,S})}]$ (**5**), respectively. Addition reaction of $\mathrm{LiCab^S}$ ($\mathrm{Cab^S = SC_2(H)B_{10}H_{10}}$) to the rhodium complex **5** yields $[\mathrm{Rh(Cp^*)(Cab^S)(Cab^{N,S})}]$ (**6**). All the complexes were characterized by IR and NMR spectroscopy, and by elemental analysis. In addition, X-ray structure analyses were performed on complexes **2**, **3**, **5**, and **6**, in which the potential C,N- and N,S-chelate ligands were found to coordinate in a bidentate mode. The carborane complex **2** shows catalytic activities up to $3.7\times10^5\,\mathrm{g\,PE\,mol^{-1}\,Ir\,h^{-1}}$ for the polymerization of ethylene in the presence of methylaluminoxane (MAO) as cocatalyst. The polymer obtained from this homogeneous catalytic reaction has a spherical morphology. Catalytic activities and the molecular weight of polyethylene have been investigated for various reaction conditions.

Keywords: carboranes · half-sandwich complexes · homogeneous catalysis · polyethylene · polymerization

Introduction

In the past few years, the interest in transition-metal complexes with ligands containing dissimilar donor atoms has increased, primarily for their application in important homogeneous catalytic processes.[1–8] Recent reports on unusually stable C,N-,[9] C,P-,[10] N,S-,[11] N,P-,[12] and S,S′-[13]chelating *o*-carboranyl metal complexes seem to imply that the rigid chelate conformation and the *ortho*-carboranyl ligand backbone might be ideal for the stabilization of possible metal intermediates in organometallic reactions. Therefore, the design of such a ligand system containing one functional group strongly bound to a transition metal center and another one coordinatively labile has been of considerable interest.[14–18]

During the course of our previous work, we found that nickel complexes containing C,N-chelate ligands show catalytic activity in the polymerization of norbornene in the presence of methylaluminoxane (MAO).[19,20] Mononuclear M(Cp*) ($\mathrm{Cp^* = \eta^5\text{-}C_5Me_5}$) half-sandwich complexes are useful model complexes, in which one hemisphere of the coordination shell is blocked by a six-electron-donor-substituted cyclopentadienyl ring. The functionalized *o*-carborane ligands can be accommodated in the remaining coordination hemisphere to form a variety of complexes. It was therefore of interest to investigate the use of such intramolecularly coordinated complexes containing the *o*-carboranyl C,N- and N,S-chelating ligand systems as catalysts for olefin polymerization.

To investigate the influence of these dissimilar chelating donor ligands on the catalytic behavior of the complexes in olefin polymerization, we synthesized and characterized half-sandwich iridium, ruthenium, and rhodium complexes containing picolyl-functionalized carboranes. Complex **2** was successfully applied as a homogeneous catalyst for the polymerization of ethylene and its catalytic activity will be discussed below.

---

[a] Dr. X. Wang, Prof. Dr. G.-X. Jin
Laboratory of Molecular Catalysis and Innovative Materials
Department of Chemistry, Fudan University
Shanghai 200433 (P. R. China)
Fax: (+86) 21-656-43776
E-mail: gxjin@fudan.edu.cn

Results and Discussion

Synthesis of half-sandwich complexes containing the C,N-ligand: 1-(2′-Picolyl)-*ortho*-carborane (**1**) was obtained by treating monolithium carborane with picolyl chloride (Scheme 1) at low temperature. IR and ^{1}H NMR spectroscopic data are consistent with the expected picolyl-*o*-carborane structure.

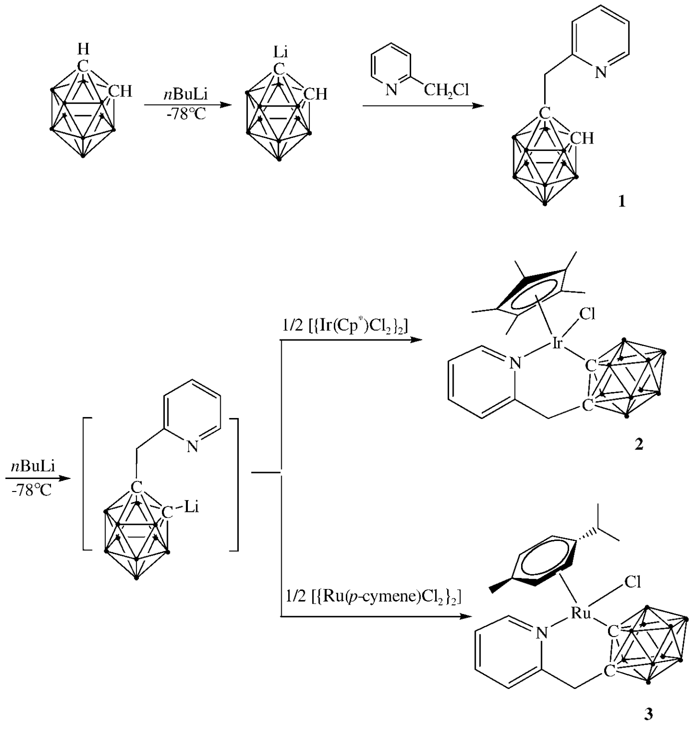

Scheme 1. Synthesis of complexes **2** and **3**.

The C,N-chelated metal complexes [Ir(Cp*)Cl(Cab$^{\mathrm{N}}$)] (**2**) and [Ru(*p*-cymene)Cl(Cab$^{\mathrm{N}}$)] (**3**) were prepared by reaction of the dimeric metal complexes [{Ir(Cp*)Cl$_2$}$_2$] and [{Ru(*p*-cymene)Cl$_2$}$_2$], respectively, with two equivalents of the corresponding lithium compound LiCab$^{\mathrm{N}}$ (Scheme 1). Complexes **2** and **3** were isolated as air-stable, orange, transparent crystals. The stability of complexes **2** and **3** is due to the formation of six-membered chelate ring. A detailed analysis of the spectroscopic data (^{1}H NMR, ^{11}B NMR, ^{13}C NMR, and IR spectra) showed that ligand **1** is coordinated to the metal center through the carbon and nitrogen atoms. The half-sandwich complexes **2** and **3** are soluble in THF and CH_2Cl_2, but only slightly soluble in hexane.

The ORTEP diagram of [Cp*IrCl(Cab$^{\mathrm{N}}$)] (**2**) is presented in Figure 1. Selected bond lengths and angles are given in Table 1. The molecular structure shows that this complex possesses a Cp*–Ir$^{\mathrm{III}}$ half-sandwich tripod structure, in which two of the "legs" are the C and N atoms from the picolyl-functionalized *o*-carborane, and the third "leg" is chloride ion. The C(2)-C(1)-Ir(1) angle of 115.4(6)° within the six-membered ring is smaller than the expected 120°. The Ir–N distance in **2** (2.130(8) Å) is longer than those found in the pyridine-containing system [Ir(Buppy)$_2$(S^S)] (S^S = Et$_2$NCS$_2$) (2.050(3) Å)[21] and in a terdentate pyridine–diimine iridium complex (1.891(5) Å).[22] The six-membered Ir-C-C-C-C-N ring is folded with a dihedral angle of 51.8° between the two planes formed by Ir(1)-C(1)-C(2)-C(3) and Ir(1)-N(1)-C(4)-C(3). The bond lengths and angles associated with picolyl and *o*-carboranyl are normal with respect to the other *o*-carboranyl-substituted compounds.[12,23,24]

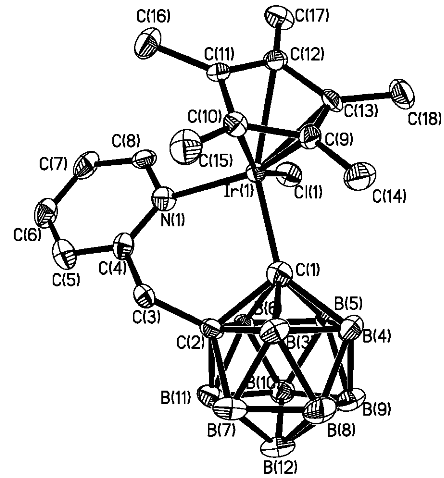

Figure 1. Molecular structure of complex **2** (hydrogen atoms omitted for clarity).

The ORTEP diagram in Figure 2 shows that the molecular structure of [(*p*-cymene)RuCl(Cab$^{\mathrm{N}}$)] (**3**) has a strong resemblance to that of complex **2**. The Ru–N distance in **3** is as expected (2.106(6) Å).[25] Both, the Ru–N and Ru–C bond lengths of 2.106(6) and 2.139(5) Å are similar to the Ir–N and Ir–C distances of complex **2**. The C(2)-C(1)-Ru(1) angle of 116.4(4)° within the six-membered ring is also smaller than the expected 120°. In complex **3** the six-membered Ru-C-C-C-C-N ring is folded with a dihedral angle of 52.6° between the two planes formed by Ru(1)-C(1)-C(2)-C(3) and Ru(1)-N(1)-C(4)-C(3), which is slightly larger than that in the corresponding iridium complex **2** (51.8°).

Synthesis of half-sandwich complexes containing the N,S-ligand: The reaction of the compound **1** with one equivalent of *n*BuLi, followed by addition of one equivalent of sulfur in THF (Scheme 2), resulted in the formation of the lithium picolylthiolate carborane LiCab$^{\mathrm{N,S}}$ (**4**; Cab$^{\mathrm{N,S}}$ = 1-(2′-picolyl)-2-lithiumthiolato-*o*-carborane). The N,S-chelated metal complex [Rh(Cp*)Cl(Cab$^{\mathrm{N,S}}$)] (**5**) was prepared by reaction between the dimeric metal complex [{Rh(Cp*)Cl$_2$}$_2$] and two equivalents of compound 4, prepared in situ (Scheme 2). Complex **5** was isolated in form of air-stable, red, transparent crystals. Starting from this steric constraint, we were interested in whether high yields of a monochelate could be obtained when **5** was treated with LiCab$^{\mathrm{S}}$ (LiCab$^{\mathrm{S}}$ = LiSC$_2$(H)B$_{10}$H$_{10}$). Thus, Cab$^{\mathrm{S}}$ easily replaces the chloride ligand in complex **5** to give the red rhodium complex **6** in good yield. The stability of complexes **5** and **6** is due to the

Table 1. Selected bond lengths (Å) and angles (°) for complexes **2** and **3**.

Complex **2**			
Ir(1)−C(1)	2.100(10)	Ir(1)−N(1)	2.130(8)
Ir(1)−C(9)	2.162(10)	Ir(1)−C(12)	2.269(9)
Ir(1)−C(10)	2.150(9)	Ir(1)−C(13)	2.163(9)
Ir(1)−C(11)	2.286(9)	Ir(1)−Cl(1)	2.416(3)
C(1)−C(2)	1.752(13)		
C(1)-Ir(1)-N(1)	88.6(4)	C(1)-Ir(1)-C(10)	112.9(4)
N(1)-Ir(1)-C(10)	105.9(3)	C(10)-Ir(1)-C(9)	38.7(3)
N(1)-Ir(1)-C(9)	143.5(4)	C(1)-Ir(1)-C(9)	98.0(4)
N(1)-Ir(1)-C(12)	115.8(3)	C(1)-Ir(1)-C(12)	155.5(4)
C(1)-Ir(1)-C(11)	150.3(4)	C(13)-Ir(1)-C(12)	38.5(4)
C(10)-Ir(1)-C(13)	64.2(4)	C(9)-Ir(1)-C(13)	37.7(4)
C(1)-Ir(1)-C(13)	117.0(4)	N(1)-Ir(1)-C(13)	154.3(3)
C(10)-Ir(1)-C(12)	62.8(3)	C(9)-Ir(1)-C(12)	63.0(4)
N(1)-Ir(1)-C(11)	95.1(3)	C(10)-Ir(1)-C(11)	37.9(3)
C(1)-Ir(1)-Cl(1)	88.7(3)	C(10)-Ir(1)-Cl(1)	155.8(3)
C(9)-Ir(1)-C(11)	62.5(3)	C(13)-Ir(1)-C(11)	62.1(3)
C(12)-Ir(1)-C(11)	35.4(3)	N(1)-Ir(1)-Cl(1)	84.6(2)
C(9)-Ir(1)-Cl(1)	131.2(3)	C(13)-Ir(1)-Cl(1)	96.9(3)
C(12)-Ir(1)-Cl(1)	93.0(3)	C(2)-C(1)-Ir(1)	115.4(6)
C(11)-Ir(1)-Cl(1)	120.9(2)		
Complex **3**			
Ru(1)−C(1)	2.106(6)	Ru(1)−N(1)	2.139(5)
Ru(1)−C(14)	2.153(6)	Ru(1)−C(12)	2.187(5)
Ru(1)−C(13)	2.168(6)	Ru(1)−C(9)	2.202(6)
Ru(1)−C(11)	2.298(6)	Ru(1)−C(10)	2.300(6)
C(1)−C(2)	1.764(8)	Ru(1)−Cl(1)	2.4118(15)
C(1)-Ru(1)-C(13)	95.2(2)	C(14)-Ru(1)-C(13)	38.4(2)
C(1)-Ru(1)-N(1)	88.2(2)	C(1)-Ru(1)-C(14)	88.9(2)
N(1)-Ru(1)-C(14)	149.6(2)	N(1)-Ru(1)-C(13)	111.9(2)
C(13)-Ru(1)-C(12)	37.4(2)	N(1)-Ru(1)-C(9)	160.8(2)
C(1)-Ru(1)-C(12)	125.4(2)	N(1)-Ru(1)-C(12)	89.4(2)
C(14)-Ru(1)-C(12)	68.0(2)	C(1)-Ru(1)-C(9)	111.0(3)
C(12)-Ru(1)-C(9)	80.2(2)	C(13)-Ru(1)-C(11)	65.4(2)
C(12)-Ru(1)-C(11)	36.3(2)	N(1)-Ru(1)-C(11)	97.1(2)
C(14)-Ru(1)-C(11)	77.0(2)	C(1)-Ru(1)-C(10)	147.7(3)
C(9)-Ru(1)-C(11)	65.2(2)	N(1)-Ru(1)-C(10)	124.0(2)
C(14)-Ru(1)-C(10)	65.3(2)	C(13)-Ru(1)-C(10)	77.0(2)
C(12)-Ru(1)-C(10)	64.4(2)	C(11)-Ru(1)-C(10)	34.1(2)
C(9)-Ru(1)-C(10)	36.8(2)	C(1)-Ru(1)-Cl(1)	87.64(17)
N(1)-Ru(1)-Cl(1)	84.79(13)	C(14)-Ru(1)-Cl(1)	125.31(18)
C(13)-Ru(1)-Cl(1)	163.16(17)	C(9)-Ru(1)-Cl(1)	94.91(16)
C(12)-Ru(1)-Cl(1)	146.30(17)	C(11)-Ru(1)-Cl(1)	111.59(16)
C(10)-Ru(1)-Cl(1)	91.77(15)		

formation of a seven-membered chelate ring. A detailed analysis of the spectroscopic data (^{1}H NMR, ^{11}B NMR, ^{13}C NMR, and IR spectra) showed that the 1-(2′-picolyl)-2-lithiumthiolato-*o*-carborane is coordinated to the metal center through the sulfur and nitrogen atoms.

The ORTEP diagram of compound **5** is presented in Figure 3. Selected bond lengths and angles are given in Table 2. The molecular structure reveals that the geometry at the rhodium(III) center is a three-legged piano-stool with the rhodium atom coordinated by the η^5-Cp*, η^2-Cab^{N,S} and chloride ligands. The coordination of the bidentate ligand Cab^{N,S} results in a seven-membered $RhNC_4S$ ring, in which Rh(1), N(1) and C(4) lie above the plane formed by the C_3S fragment C(3)-C(2)-C(1)-S(1) (Rh(1) 0.2875 Å, N(1) 0.4391 Å, C(4) 0.2948 Å). The Rh−S distance (2.3889(17) Å)

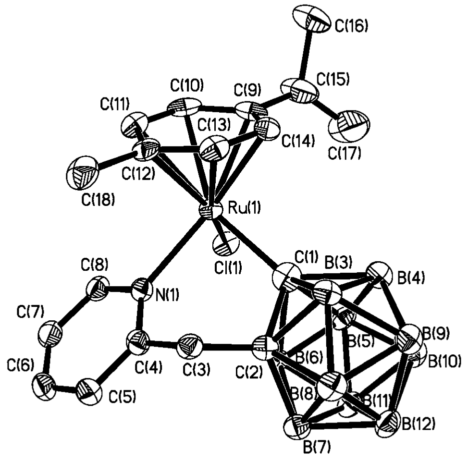

Figure 2. Molecular structure of complex **3** (hydrogen atoms omitted for clarity).

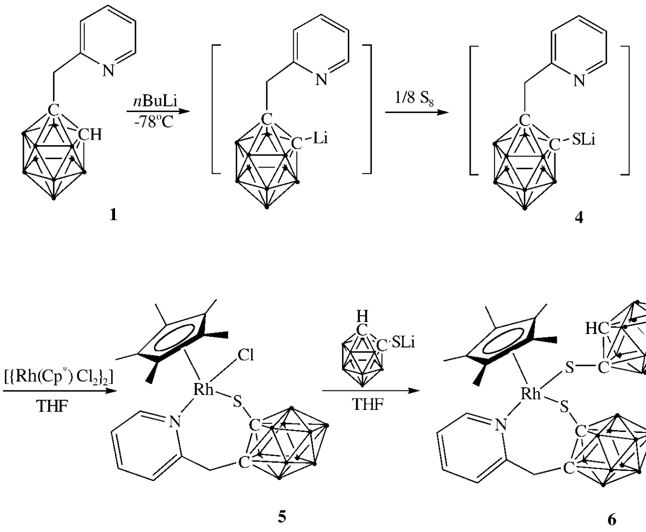

Scheme 2. Synthesis of complexes **5** and **6**.

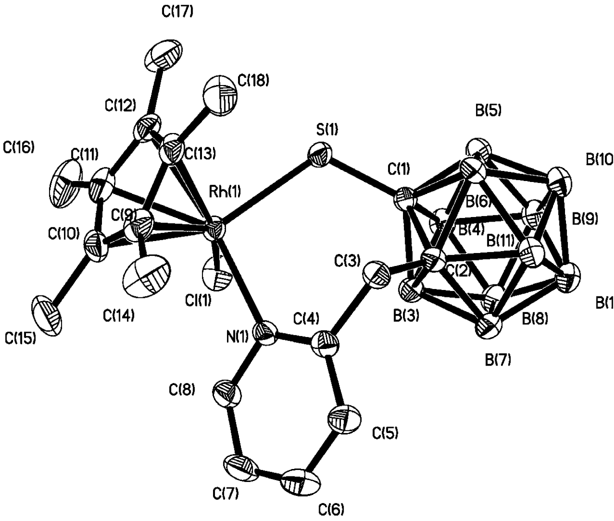

Figure 3. Molecular structure of complex **5** (hydrogen atoms omitted for clarity).

Table 2. Selected bond lengths (Å) and angles (°) for complexes **5** and **6**.

Complex **5**			
Rh(1)–N(1)	2.151(2)	Rh(1)–C(13)	2.151(3)
Rh(1)–C(12)	2.153(3)	Rh(1)–C(9)	2.164(3)
Rh(1)–C(10)	2.172(3)	Rh(1)–C(11)	2.179(3)
Rh(1)–S(1)	2.3925(9)	Rh(1)–Cl(1)	2.4036(9)
C(1)–C(2)	1.695(4)		
N(1)-Rh(1)-C(13)	116.72(11)	N(1)-Rh(1)-C(12)	154.34(10)
C(13)-Rh(1)-C(12)	38.95(12)	N(1)-Rh(1)-C(9)	90.53(10)
C(13)-Rh(1)-C(9)	38.44(12)	C(12)-Rh(1)-C(9)	64.58(12)
C(9)-Rh(1)-C(10)	38.25(13)	N(1)-Rh(1)-C(11)	137.04(12)
C(13)-Rh(1)-C(11)	63.93(11)	C(12)-Rh(1)-C(11)	37.86(12)
C(9)-Rh(1)-C(11)	63.74(13)	C(10)-Rh(1)-C(11)	38.06(13)
N(1)-Rh(1)-C(10)	100.64(11)	C(13)-Rh(1)-C(10)	64.26(11)
C(12)-Rh(1)-C(10)	64.17(12)	N(1)-Rh(1)-S(1)	101.46(6)
C(13)-Rh(1)-S(1)	91.88(8)	C(12)-Rh(1)-S(1)	89.50(9)
N(1)-Rh(1)-Cl(1)	88.58(7)	C(11)-Rh(1)-S(1)	121.46(10)
C(10)-Rh(1)-S(1)	153.02(9)	C(9)-Rh(1)-Cl(1)	141.66(10)
C(12)-Rh(1)-Cl(1)	114.56(9)	C(13)-Rh(1)-Cl(1)	153.25(9)
S(1)-Rh(1)-Cl(1)	91.29(4)	C(11)-Rh(1)-Cl(1)	91.99(9)
C(10)-Rh(1)-Cl(1)	104.55(9)	C(9)-Rh(1)-S(1)	126.31(9)
Complex **6**			
Rh(1)–N(1)	2.167(5)	Rh(1)–C(13)	2.173(6)
Rh(1)–C(14)	2.193(6)	Rh(1)–C(15)	2.188(6)
Rh(1)–C(11)	2.195(6)	Rh(1)–C(12)	2.213(6)
Rh(1)–S(1)	2.3889(17)	Rh(1)–S(2)	2.4030(15)
C(1)–C(2)	1.695(8)		
N(1)-Rh(1)-C(13)	102.4(2)	N(1)-Rh(1)-C(15)	147.6(2)
N(1)-Rh(1)-C(14)	139.9(2)	C(13)-Rh(1)-C(15)	63.5(2)
C(13)-Rh(1)-C(14)	37.7(2)	C(15)-Rh(1)-C(14)	37.7(2)
N(1)-Rh(1)-C(11)	109.8(2)	C(13)-Rh(1)-C(11)	63.8(2)
C(14)-Rh(1)-C(11)	63.3(2)	C(13)-Rh(1)-C(12)	37.5(2)
C(15)-Rh(1)-C(11)	38.1(2)	N(1)-Rh(1)-C(12)	87.9(2)
C(15)-Rh(1)-C(12)	63.0(2)	C(14)-Rh(1)-C(12)	62.4(2)
N(1)-Rh(1)-S(1)	85.08(14)	C(15)-Rh(1)-S(1)	123.82(18)
C(11)-Rh(1)-C(12)	38.0(2)	C(13)-Rh(1)-S(1)	96.37(17)
C(14)-Rh(1)-S(1)	93.87(18)	C(11)-Rh(1)-S(1)	156.89(17)
N(1)-Rh(1)-S(2)	101.89(13)	C(15)-Rh(1)-S(2)	89.38(17)
C(12)-Rh(1)-S(1)	129.88(18)	C(13)-Rh(1)-S(2)	152.88(16)
C(11)-Rh(1)-S(2)	96.44(17)	C(14)-Rh(1)-S(2)	117.89(18)
C(12)-Rh(1)-S(2)	132.41(18)	S(1)-Rh(1)-S(2)	97.53(6)

is within the range of known values for Rh–S bonds in analogous complexes.[26] The rhodium complex **5** has a Rh–N bond length (2.151(5) Å) similar to the M–N distances in the iridium complex **2** and the ruthenium complex **3**.

The structure of **6** was unambiguously established by single-crystal X-ray analysis and is shown in Figure 4. Selected bond lengths and angles are given in Table 2. Complex **6** has a similar structure to complex **5**, except that the chloride ligand is replaced by the sterically more demanding ligand Cab^S. The S(2)-Rh(1)-S(1) angle in **6** (97.53(6)°) is larger than the S(1)-Rh(1)-Cl(1) angle in the precursor **5** (91.29(4)°) and, consequently, the N(1)-Rh(1)-S(1) angle in **6** (85.08(14)°) is smaller than the N(1)-Rh(1)-Cl(1) angle in **5** (88.58(7)°); this is probably the result of the space requirement of the bulky Cab^S ligand. The chelate ligand Cab^{N,S} and the monodentate ligand Cab^S have similar Rh–S bond lengths (2.3889(17) Å in **5**, 2.4030(15) Å in **6**).

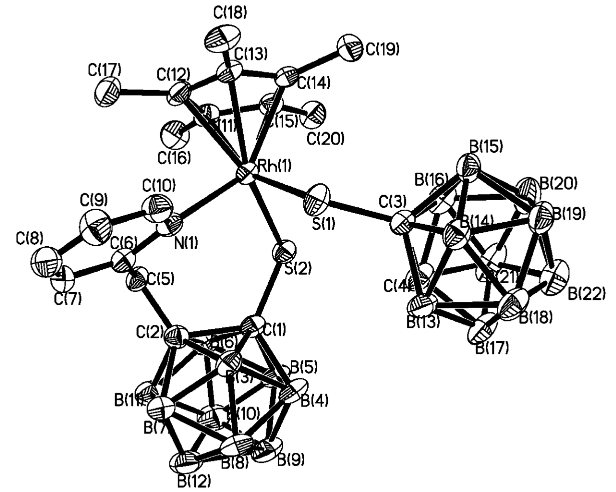

Figure 4. Molecular structure of complex **6** (hydrogen atoms omitted for clarity).

Ethylene polymerization: Preliminary experiments indicated that the iridium complex **2** can be activated by treatment with MAO to polymerize ethylene. The ethylene polymerization results are collected in Table 3, the catalytic activities for which lie in the range of 10^5 gPEmol^{-1}Irh^{-1}. The polyethylene (PE) obtained was of very high molecular weight ($M_w = 10^6$ gmol^{-1}). We found that complex **2** showed its highest activity at 30 °C (3.7×10^5 gPEmol^{-1}Irh^{-1}). Under the same conditions, neither the complex itself nor MAO produced any polymer (runs 6 and 7). The activity of **2** increased with the polymerization temperature rising from 0 °C to 30 °C; this is due to the increasing concentration of metal centers activated by MAO. However, the activated complex becomes more unstable at higher temperature, so that the highest activity found at 30 °C is the result of a compromise between these two factors. At 40 °C the activity already decreases because of the further increasing decomposition rate of the active centers. Initial attempts to measure the molecular weight of the obtained PE failed due to its

Table 3. Polymerization of ethylene with the iridium complex **2** activated by methylaluminoxane (MAO).[a]

Run	Complex	Al/Ir	T [°C]	Activity[b]	M_w[c]
1	**2**	2000	0	0.6	1.54
2	**2**	2000	20	2.6	2.17
3	**2**	2000	30	3.7	2.53
4	**2**	2000	40	2.5	2.37
5	**2**	2000	50	1.2	1.9
6[d]	**2**	–	30	0	0
7[e]	–	–	30	0	0

[a] Polymerization conditions: solvent, toluene; total volume, 50 mL; iridium complex **2**, 4 µmol; ethylene; reaction time, 30 min. [b] $\times 10^5$ gPEmol^{-1}Irh^{-1}. [c] M_w ($\times 10^{-6}$ gmol^{-1}) measured by the calibrated Ubbelohde viscosimeter technique and extrapolation to the intrinsic viscosity. [d] Without cocatalyst MAO. [e] Without iridium complex but with MAO present.

poor solubility in trichlorobenzene caused by the high molecular weight. Therefore, we measured the molecular weight by the calibrated Ubbelohde viscosimeter technique. Clearly the molecular weight is lower at higher temperature; a molecular weight of 2.53×10^6 g mol^{-1} was obtained at a reaction temperature of 30 °C.

The spherical morphology of polyethylene obtained from the reaction catalyzed by the homogeneous catalyst [Ir(Cp*)Cl(Cab^N)] (**2**) (see Figure 5) is different from the sponge-like morphology catalyzed in which other homogeneous catalysts are used.[27]

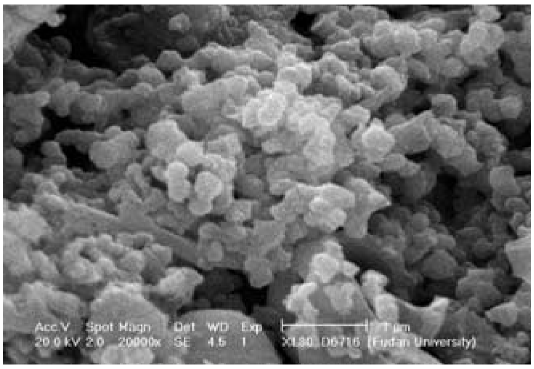

Figure 5. SEM image of polyethylene obtained with [Ir(Cp*)Cl(Cab^N)] as catalyst.

Conclusion

This report presents the first intramolecularly coordinated half-sandwich complexes containing an *o*-carboranyl C,N- or N,S-chelating ligand system. A combination of X-ray crystallographic and spectroscopic studies confirmed the structure of these half-sandwich complexes. A preliminary study showed that the new half-sandwich iridium complex **2** is the precursor for a catalyst moderately active in ethylene polymerization. To the best of our knowledge, this is the first report on N-functionalized *o*-carboranyl half-sandwich metal complexes exhibiting activity toward polymerization of ethylene.

Experimental Section

General data: All manipulations were performed under an atmosphere of argon using standard Schlenk techniques. CH_2Cl_2 was dried over CaH_2, THF, diethyl ether, hexane, and toluene were dried over Na, and then distilled under nitrogen atmosphere immediately prior to use. Methylaluminoxane (MAO) and 2-picolyl chloride hydrochloride were purchased from Witco and Acros, respectively. Other chemicals were of technical grade and were used as received. [{Ir(Cp*)Cl_2}$_2$],[28] [{Rh(Cp*)Cl_2}$_2$],[28] and [{Ru(*p*-cymene)Cl_2}$_2$]$_2$[29] were prepared according to literature procedures. ^{1}H, ^{13}C, and ^{11}B NMR spectra were recorded in $CDCl_3$ on a VAVCE-DMX 500 Spectrometer. Elemental analyses were performed on an Elementar vario EL III Analyzer. The molecular weight (M_w) of PE was measured by the calibrated Ubbelohde viscosimeter technique and extrapolation to the intrinsic viscosity. IR spectra (KBr) were recorded on the Nicolet FT-IR spectrophotometer.

Synthesis of 1-(2′-picolyl)-*ortho*-carborane (1): *n*BuLi in hexane (2.5 M, 0.8 mL, 2 mmol) was added to a solution of *ortho*-carborane (288 mg, 2 mmol) in Et_2O (20 mL) at −78 °C, and the reaction mixture was stirred for 1 h at −78 °C. Then 2-picolyl chloride (255 mg, 2 mmol, prepared by neutralizing picolyl chloride hydrochloride) was added at −78 °C and the stirred reaction mixture was allowed to warm to room temperature for 1 h. Addition of water (30 mL) dissolved the nascent LiCl; the Et_2O layer was separated and further washed with water (2×30 mL) before drying over Na_2SO_4. Filtration followed by removal of the solvent under vacuum yielded a white solid. Unreacted *ortho*-carborane was removed by slow vacuum sublimation (40 °C, 0.01 mmHg) to give analytically pure **1** (250 mg, 57 % yield). ^{1}H NMR (500 MHz, $CDCl_3$): $\delta=8.56$ (d, 1H; pyridyl), 7.70 (m, 1H; pyridyl), 7.26 (m, 1H; pyridyl), 7.18 (d, 1H; pyridyl), 4.08 (s, 1H; C(1)H), 3.66 (m, 1H; CH_2), 3.55 ppm (m, 1H; CH_2); IR (KBr): $\tilde{\nu}=3069$, 3020 (br m; carborane CH), 2916 (w), 2848 (w; pyridyl/CH_2), 2596 (vs), 2575 cm^{-1} (s; BH).

Synthesis of [Ir(Cp*)Cl(Cab^N)] (2): *n*BuLi (2.5 M, 0.4 mL, 1 mmol) was added through a syringe to a stirred solution of **1** (120 mg, 1 mmol) in THF (20 mL) cooled to −78 °C. The resulting pale-yellow solution was stirred at room temperature for 1 h and then transferred by means of a cannula to a suspension of [{Ir(Cp*)Cl_2}$_2$] (400 mg, 0.5 mmol) in THF (20 mL). After stirring for 16 h, the solvent was removed under vacuum; the resulting residue was redissolved in a minimum of CH_2Cl_2 and then recrystallized by slow diffusion of hexane into this solution. Yield: 370 mg (62 %); ^{1}H NMR (500 MHz, $CDCl_3$): $\delta=9.18$ (m, 1H; pyridyl), 7.72 (m, 1H; pyridyl), 7.15 (m, 2H; pyridyl), 3.67 (m, 1H; CH_2), 3.40 (m, 1H; CH_2), 1.68 ppm (s, 15H; $C_5(CH_3)_5$); ^{13}C NMR (125 MHz, $CDCl_3$): $\delta=159.6$ (pyridyl, C2), 158.2 (pyridyl, C6), 138.4 (pyridyl, C4), 125.8 (pyridyl, C5), 125.3 (pyridyl, C3), 89.9 ($C_5(CH_3)_5$), 52.1 (C_2B_{10}), 49.2 (NCH_2), 9.17 ppm ($C_5(CH_3)_5$); ^{11}B NMR (160 MHz, $CDCl_3$): $\delta=-4.54$ (1B), −6.55 (1B), −7.99 (2B), −10.79 (2B), −11.56 (2B), −13.85 ppm (2B); IR (KBr): $\tilde{\nu}=3057$ (br m; carborane CH), 2924 (w), 2850 (w; pyridyl/CH_2), 2561 cm^{-1} (vs; BH); elemental analysis calcd (%) for $C_{18}H_{31}B_{10}ClIrN$: C 36.20, H 5.20, N 2.35; found: C 36.18, H 5.29, N 2.34.

Synthesis of [Ru(*p*-cymene)Cl(Cab^N)] (3): *n*BuLi (2.5 M, 0.4 mL, 1 mmol) was added through a syringe to a stirred solution of **1** (235 mg, 1 mmol) in THF (20 mL) cooled to −78 °C. The resulting pale-yellow solution was stirred at room temperature for 1 h and then transferred by means of a cannula to a suspension of [{Ru(*p*-cymene)Cl_2}$_2$] (306 mg, 0.5 mmol) in THF (20 mL). After stirring for 16 h, the solvent was removed under vacuum; the resulting residue redissolved in a minimum of CH_2Cl_2 and then recrystallized by slow diffusion of hexane into this solution. Yield: 222 mg (44 %); ^{1}H NMR (500 MHz, $CDCl_3$): $\delta=9.18$ (m, 1H; pyridyl), 7.72 (m, 1H; pyridyl), 7.22 (m, 2H; pyridyl), 5.63 (m, 4H; C_6H_4), 3.55 (m, 2H; CH_2), 2.76 (m, 1H; CH), 2.04 (m, 3H; CH_3), 1.13 ppm (m, 6H; $CH(CH_3)_2$); ^{11}B NMR (160 MHz, $CDCl_3$): $\delta=-2.61$ (2B), −9.46 (2B), −13.91 (4B), −15.06 ppm (2B); IR (KBr): $\tilde{\nu}=3003$ (br m; carborane CH), 2954 (w), 2908 (w; pyridyl/CH_2), 2576 cm^{-1} (vs; BH); elemental analysis calcd (%) for $C_{18}H_{30}B_{10}ClNRu$: C 42.81, H 5.94, N 2.77; found: C 42.35, H 5.62, N 2.44.

Synthesis of [Rh(Cp*)Cl(Cab^{N,S})] (5): *n*BuLi (2.5 M, 0.4 mL, 1 mmol) was added through a syringe to a stirred solution of **1** (235 mg, 1 mmol) in hexane (20 mL) at −10 °C. The resulting mixture was stirred for 4 h at room temperature, before the formed white precipitate was separated from the solution by decantation. The obtained solid LiCab^{N,S} was washed with hexane (2×20 mL), dried under vacuum, dissolved in THF (20 mL), and slowly added to a suspension of sublimed sulfur (32 mg, 1 mmol) in THF (15 mL). The mixture was stirred for 4 h and transferred by means of a cannula to a suspension of [{Rh(Cp*)Cl_2}$_2$] (309 mg, 0.5 mmol) in THF (20 mL). After stirring for 16 h, the solvent was removed under vacuum, the resulting residue redissolved in a minimum of CH_2Cl_2, and then recrystallized by slow diffusion of hexane into this solution. Yield: 394 mg (73 %); ^{1}H NMR (500 MHz, $CDCl_3$): $\delta=9.34$ (m, 1H; pyridyl), 7.89 (m, 1H; pyridyl), 7.41 (m, 1H; pyridyl), 7.26 (m, 1H; pyridyl), 4.37 (m, 1H; CH_2), 3.79 (m, 1H; CH_2), 1.46 ppm (s, 15H; $C_5(CH_3)_5$); ^{13}C NMR (500 MHz, $CDCl_3$): $\delta=159.8$ (pyridyl, C2), 155.9 (pyridyl, C6), 138.8 (pyridyl, C4), 126.9 (pyridyl, C5), 124.7 (pyridyl, C3), 95.6 ($C_5(CH_3)_5$), 53.5 (C_2B_{10}), 43.68 (NCH_2), 8.47 ppm ($C_5(CH_3)_5$); ^{11}B NMR (160 MHz, $CDCl_3$): $\delta = -4.62$ (1B), −7.99 (4B), −11.31 (4B), −13.29 ppm (1B); IR (KBr): $\tilde{\nu} = 3029$ (br m; carborane CH), 2944 (w), 2915 (w; pyridyl/CH_2), 2567 cm^{-1} (vs; BH); elemental analysis calcd (%) for $C_{18}H_{31}B_{10}ClNRhS \cdot 2\,CH_2Cl_2$: C 33.83, H 4.93, N 1.98; found: C 33.68, H 4.77, N 1.66.

Synthesis of [Cp*Rh(Cab^{N,S})(Cab^S)] (6): *n*BuLi (2.5 M, 0.2 mL, 0.5 mmol) was added through a syringe to a stirred solution of *ortho*-carborane (72 mg, 0.5 mmol) in Et_2O (20 mL) at −10 °C. The resulting mixture was stirred for 1 h at room temperature and then slowly added to suspension of sublimed sulfur (16 mg, 0.5 mmol) in THF (10 mL). The solution was stirred for 2 h and transferred by means of a cannula to a solution of **5** (270 mg, 0.5 mmol) in THF (20 mL). After stirring for 16 h, the solvent was removed under vacuum; the resulting residue redissolved in a minimum of CH_2Cl_2 and then recrystallized by slow diffusion of hexane into this solution. Yield: 282 mg (83 %); ^{1}H NMR (500 MHz, $CDCl_3$): $\delta = 9.32$ (m, 1H; pyridyl), 7.76 (m, 1H; pyridyl), 7.33 (m, 1H; pyridyl), 7.21 (m, 1H; pyridyl), 4.33 (m, 1H; CH_2), 3.65 (m, 1H; CH_2), 1.63 ppm (s, 15H; $C_5(CH_3)_5$); ^{11}B NMR (160 MHz, $CDCl_3$): $\delta = -5.67$ (2B), −7.41 (2B), −8.80 (4B), −9.35 (4B), −10.95 (4B), −12.11 (2B), −13.84 ppm (2B); IR (KBr): $\tilde{\nu} = 3022$ (br m; carborane CH), 2964 (w), 2915 (w; pyridyl/CH_2); 2576 cm^{-1} (vs, BH); elemental analysis calcd (%) for $C_{20}H_{42}B_{20}NRhS_2 \cdot 1.5\,CH_2Cl_2$: C 31.90, H 5.58, N 1.73; found: C 31.70, H 5.54, N 1.67.

X-ray crystallography: Crystals suitable for single-crystal X-ray analysis of **2**, **3**, **5**, and **6** were obtained by slow diffusion of hexane into a solution of the corresponding compound in CH_2Cl_2. Diffraction data of **2**, **3**, **5**, and **6** were collected at 293 K on a Bruker Smart APEX CCD diffractometer ($Mo_{K\alpha}$ radiation). None of the crystals showed signs of decomposition during the X-ray data collection carried out at room temperature ($\lambda = 0.71073$ Å). Details of the data collection and refinement are summarized in Table 4. Selected bond lengths and angles are given in Tables 1 and 2. The structures were solved by direct methods by using SHELXS-97[30] and refined by full-matrix least-square calculations on F^2 by using SHELXTL-97.[30]

CCDC-262025 (**2**), CCDC-262026 (**3**), CCDC-262027 (**5**), and CCDC-262028 (**6**) contain the supplementary crystallographic data for this paper. These data can be obtained free of charge from The Cambridge Crystallographic Data Centre via www.ccdc.cam.ac.uk/data_request/cif.

Ethylene polymerization: Ethylene polymerization with the iridium catalyst was performed at 1 atm of ethylene pressure in a 200 mL Schlenk-type glass reactor fitted with a mechanical stirrer. After being flame-dried three times, the flask was back-filled with ethylene. Then the reactor was charged with toluene (45 mL) and MAO (10 %) by means of a syringe under an atmosphere of nitrogen. The reaction flask was immersed in a water bath at a specific temperature for 15 min prior to injection of the catalyst. The catalyst dissolved in toluene (5 mL) was introduced into the polymerization bottle by means of a syringe, stirring was started, and the polymerization was kept at the desired temperature. After 30 minutes, the polymerization was quenched with ethanol/HCl, the polymer was isolated by filtration and dried under vacuum at 40 °C for 10 h.

Acknowledgements

Financial support by the National Nature Science Foundation of China for Distinguished Young Scholars (29925101, 20421303) and by the special Funds for Major State Basic Research Projects (G 1999064800) is gratefully acknowledged.

Table 4. Summary of crystallographic data for compounds **2**, **3**, **5**, and **6**.

	2	**3**	**5**	**6**
formula	$C_{18}H_{31}B_{10}ClIrN$	$C_{18}H_{30}B_{10}ClNRu$	$C_{19}H_{33}B_{10}Cl_3NRhS$	$C_{23}H_{49}B_{20}NRhS_2$
M_r	597.19	505.05	624.88	720.86
T [K]	293(2)	293(2)	293(2)	293(2)
crystal system	triclinic	monoclinic	monoclinic	monoclinic
space group	$P\bar{1}$	$P2_1/n$	$P2_1/n$	$P2_1/n$
a [Å]	7.842(2)	11.135(4)	11.092(4)	11.6549(19)
b [Å]	10.295(3)	16.558(6)	16.052(5)	12.349(2)
c [Å]	15.825(4)	13.145(5)	16.256(5)	26.378(4)
α [°]	75.445(4)	90	90	90
β [°]	85.084(4)	108.568(5)	98.435(4)	90.948(3)
γ [°]	71.090(4)	90	90	90
V [Å^3]	1170.0(5)	2297.4(14)	2863.0(16)	3796.0(11)
Z	2	4	4	4
ρ_{calcd} [Mg m^{-3}]	1.695	1.460	1.450	1.265
μ [mm^{-1}]	5.828	0.806	0.961	0.580
$F(000)$	580	1024	1264	1484
crystal size [mm^3]	0.10 × 0.05 × 0.05	0.10 × 0.10 × 0.05	0.25 × 0.20 × 0.15	0.10 × 0.08 × 0.05
θ range [°]	2.15–25.01	2.05–26.01	1.79–26.01	1.54–25.01
limiting indices	$-7 \leq h \leq 9$,	$-13 \leq h \leq 13$,	$-13 \leq h \leq 13$,	$-11 \leq h \leq 13$,
	$-7 \leq k \leq 12$,	$-20 \leq k \leq 9$,	$-19 \leq k \leq 19$,	$-13 \leq k \leq 14$,
	$-18 \leq l \leq 18$	$-16 \leq l \leq 15$	$-19 \leq l \leq 11$	$-31 \leq l \leq 31$
reflections collected	4973	10332	12463	15628
independent reflections	4081 [R(int) = 0.0328]	4496 [R(int) = 0.0678]	5599 [R(int) = 0.0179]	6678 [R(int) = 0.0705]
completeness to θ [%]	98.7	99.6	99.4	99.9
max/min transmission	0.7593/0.5934	0.9608/0.9237	0.8692/0.7951	0.9716/0.9443
data/restraints/parameters	4081/0/290	4496/0/290	5599/0/326	6678/0/428
goodness-of-fit on F^2	1.069	1.040	0.742	1.014
final R indices [$I > 2\sigma(I)$]	$R1 = 0.0506$	$R1 = 0.0540$	$R1 = 0.0295$	$R1 = 0.0618$
	$wR2 = 0.1077$	$wR2 = 0.1183$	$wR2 = 0.0792$	$wR2 = 0.1351$
largest diff peak/hole [e Å^{-3}]	1.907/−1.392	1.232/−0.658	0.749/−0.320	1.006/−0.397

---

[1] I. Takei, Y. Nishibayashi, Y. Arikawa, S. Uemura, M. Hidai, *Organometallics* **1999**, *18*, 2271–2274.

[2] M. Valentini, K. Selvakumar, M. Woerle, P. S. Pregosin, *J. Organomet. Chem.* **1999**, *587*, 244–251.
[3] I. D. Kostas, C. G. Screttas, *J. Organomet. Chem.* **1999**, *585*, 1–6.
[4] A. Jacobi, G. Huttner, U. Winterhalter, *J. Organomet. Chem.* **1998**, *571*, 231–241.
[5] H. Yang, M. Alvarez-Gressier, N. Lugan, R. Mathieu, *Organometallics* **1997**, *16*, 1401–1409.
[6] H. Yang, N. Lugan, R. Mathieu, *Organometallics* **1997**, *16*, 2089–2095.
[7] Y. Hayashi, H. Sakai, N. Kaneta, M. Uemura, *J. Organomet. Chem.* **1995**, *503*, 143–148.
[8] C. G. Arena, F. Nicolo, D. Drommi, G. Bruno, F. Faraone, *J. Chem. Soc. Chem. Commun.* **1994**, 2251–2252.
[9] J. D. Lee, S. J. Kim, D. Yoo, J. Ko, S. Cho, S. O. Kong, *Organometallics* **2000**, *19*, 1695–1703.
[10] T. Lee, S. W. Lee, H. G. Wang, J. Ko, S. O. Kang, *Organometallics* **2001**, *20*, 741–748.
[11] S. W. Chung, J. Ko, K. Park, S. Cho, S. O. Kang *Collect. Czech. Chem. Commun.* **1999**, *64*, 883–894.
[12] H.-S. Lee, J.-Y. Bae, J. Ko, Y. S. Kang, H. S. Kim, S.-J. Kim, J.-H. Chung, S. O. Kang, *J. Organomet. Chem.* **2000**, *614–615*, 83–91.
[13] a) G.-X. Jin, *Coord. Chem. Rev.* **2004**, *246*, 587–602; b) X. Y. Yu, S. X. Lu, G.-X. Jin, *Inorg. Chim. Acta* **2004**, *357*, 361–366; c) X. Y. Yu, G.-X. Jin, N. H. Hu, L. H. Weng, *Organometallics* **2002**, *21*, 5540–5548; d) G.-X. Jin, J.-Q. Wang, Z. Zheng, L. H. Weng, M. Herberhold, *Angew. Chem.* **2005**, *117*, 264–267; *Angew. Chem. Int. Ed.* **2005**, *44*, 259–262; e) J.-Q. Wang, X. F. Hou, L. H. Weng, G.-X. Jin, *Organometallics* **2005**, *24*, 826–830; f) J.-Q. Wang, L. H. Weng, G.-X. Jin, *J. Organomet. Chem.* **2005**, *690*, 249–252.
[14] a) D. M. Roundhill, R. A. Bechtold, S. G. N. Roundhill, *Inorg. Chem.* **1980**, *19*, 284–289; b) T. B. Rauchfuss, F. T. Patino, D. M. Roundhill, *Inorg. Chem.* **1975**, *14*, 652–656.
[15] a) P. W. N. M. van Leeuwen, P. C. J. Kamer, J. N. H. Reek, P. Dierkes, *Chem. Rev.* **2000**, *100*, 2741–2770; b) K. Issleib, D. Mueller, *Chem. Ber.* **1959**, *92*, 3175–3182.
[16] D. S. McGuinness, K. J. Cavell, *Organometallics* **2000**, *19*, 741–748.
[17] J. C. C. Chen, I. J. B. Lin, *Organometallics* **2000**, *19*, 5113–5121.
[18] M. Gandelman, D. Milstein, *Chem. Commun.* **2000**, 1603–1604.
[19] X. Wang, S. Liu, G.-X. Jin, *Organometallics* **2004**, *23*, 6002–6007.
[20] X. Wang, G.-X. Jin, *Organometallics* **2004**, *23*, 6319–6322.
[21] M.-K. Lau, K.-M. Cheung, Q.-F. Zhang, Y. L. Song, W.-T. Wong, I. D. Williams, W. H. Leung, *J. Organomet. Chem.* **2004**, *689*, 2401–2410.
[22] S. Nuckel, P. Burger, *Organometallics* **2001**, *20*, 4345–4359.
[23] J. D. Lee, C. K. Baek, J. Ko, K. Park, S. Cho, S.-K. Min, S. O. Kang, *Organometallics* **1999**, *18*, 2189–2197.
[24] H. Wang, H. P. Wang, H. W. Li, Z. W. Xie, *Organometallics* **2004**, *23*, 875–885.
[25] a) D. Sellman, K. Hein, F. W. Heinemann, *Eur. J. Inorg. Chem.* **2004**, 3136–3146; b) P. C. Wu, J. K. Yu, Y. H. Song, Y. Chi, P. T. Chou, S. M. Peng, G. H. Lee, *Organometallics* **2003**, *22*, 4938–4946.
[26] a) H. S. Lee, J. Y. Bae, D. H. Kim, H. S. Kim, S. J. Kim, S. Cho, J. Ko, S. O. Kang, *Organometallics* **2002**, *21*, 210–219; b) H. S. Lee, J. Y. Bae, J. Ko, S. O. Kang, *Chem. Lett.* **2000**, 602–603.
[27] a) K. S. Lee, C. G. Oh, J. H. Yim, S. K. Ihm, *J. Mol. Catal. A* **2000**, *159*, 301–308; b) C. Guo, G.-X. Jin, F. Wang, *J. Polym. Sci. Part A* **2004**, *42*, 4830–4837.
[28] C. White, A. Yates, P. M. Maitlis, *Inorg. Synth.* **1992**, *29*, 228–230.
[29] M. A. Bennett, A. K. Smith, *J. Chem. Soc. Dalton Trans.* **1974**, 233–241.
[30] G. M. Sheldrick, SHELXL-97, program for the refinement of crystal structures, University of Göttingen, Göttingen, Germany, 1997.

Received: March 14, 2005